5262–5270 *Nucleic Acids Research, 2012, Vol. 40, No. 12* *Published online 25 February 2012*
doi:10.1093/nar/gks158

CTCF binds to sites in the major histocompatibility complex that are rapidly reconfigured in response to interferon-gamma

Diego Ottaviani[1], Elliott Lever[1,2], Shihong Mao[3], Rossitza Christova[1], Babatunji W. Ogunkolade[1], Tania A. Jones[1], Jaroslaw Szary[1], Johan Aarum[1], Muhammad A. Mumin[1], Christopher A. Pieri[1], Stephen A. Krawetz[3,*] and Denise Sheer[1,*]

[1]Blizard Institute, Barts and the London School of Medicine and Dentistry, Queen Mary University of London, Newark St, London E1 2AT, UK, [2]University College London Medical School, Gower Street, London, UK and [3]The Center for Molecular Medicine and Genetics and Department of Obstetrics and Gynecology, Wayne State University School of Medicine, C.S. Mott Center, Detroit, MI 48201, USA

Received May 15, 2011; Revised January 26, 2012; Accepted January 28, 2012

ABSTRACT

Activation of the major histocompatibility complex (MHC) by interferon-gamma (IFN−γ) is a fundamental step in the adaptive immune response to pathogens. Here, we show that reorganization of chromatin loop domains in the MHC is evident within the first 30 min of IFN−γ treatment of fibroblasts, and that further dynamic alterations occur up to 6 h. These very rapid changes occur at genomic sites which are occupied by CTCF and are close to IFN−γ-inducible MHC genes. Early responses to IFN−γ are thus initiated independently of CIITA, the master regulator of MHC class II genes and prepare the MHC for subsequent induction of transcription.

INTRODUCTION

The major histocompatibility complex (MHC) is considered the most important genomic region in adaptive and innate immunity, autoimmunity and disease susceptibility (1,2). The locus is remarkable in that its linear organization into sub-regions containing gene clusters facilitates highly efficient and coordinated regulation of gene expression (3). These sub-regions—class I (telomeric), class III, class II and extended class II (centromeric)—contain discrete gene families derived from genomic duplications during evolution (1). The MHC class I and II regions contain genes encoding HLA molecules which present antigens to T-cells, while the class III region contains complement, inflammatory and stress response genes. Most of the class I HLA genes and the class III genes are constitutively expressed in all somatic cells, whereas the class II HLA genes are expressed only in specialized cells in the thymus and dedicated antigen presenting cells (4). In all other cell types, interferon-gamma (IFN−γ) and other cytokines up-regulate MHC class II genes to ensure that a full T-cell response is generated.

IFN−γ is synthesized by a variety of immune cells, including CD4+ T_H1 cells, CD8+ cytotoxic lymphocytes and natural killer cells in response to mitogenic and antigenic stimuli (5). In non-antigen presenting cells, IFN−γ induction of MHC expression is initiated by JAK-STAT signalling from the IFN−γ receptor to a cascade that elicits expression of specific transcription factors (4,6). These include CIITA, which is recruited to the constitutively bound enhanceosome at promoters of the class I and II HLA genes. CIITA, in turn, recruits histone acetyltransferases and histone deacetylases to the chromatin. The whole process takes several hours, with MHC class II mRNA only detectable after ~6 h of IFN−γ exposure (7). However, a massive spatial reconfiguration of chromatin is evident within the first 10 min of IFN−γ induction, where the entire MHC emerges from the chromosome territory in a giant chromatin loop (8,9). This emphasizes the importance of understanding not only the signalling cascades, but also the chromatin alterations that are rapidly triggered by IFN−γ.

Long-range promoter–enhancer interactions that are required for MHC class II gene expression have been observed after 12 h treatment with IFN−γ, by which time transcriptional induction is well established (10,11). A more extensive spatial reconfiguration has been identified at 24 h

*To whom correspondence should be addressed. Tel: +44 20 7882 2595; Fax: +44 20 7882 2180; Email: d.sheer@qmul.ac.uk
Correspondence may also be addressed to Stephen A. Krawetz. Tel: +1 313 577 6770; Fax: +1 313 577 8554; Email: steve@compbio.med.wayne.edu

The authors wish it to be known that, in their opinion, the first three authors should be regarded as joint First Authors.

of IFN−γ treatment where a large number of genomic anchors, also known as matrix attachment regions, form in the MHC class I and II regions, with significant enrichment around inducible genes (12). Genomic anchors tether chromatin to create folds and loops, and bring distal genomic regions such as promoters and enhancers together. They are therefore likely to represent a regulatory mechanism that is widespread across the MHC (13–15). There are no studies to date on chromatin changes that occur at the early stages of IFN−γ induction.

Here, we studied chromatin organization across the MHC in MRC5 fibroblasts at 30 min and 6 h of IFN−γ treatment. Detailed maps of genomic anchors at these time points were compared to untreated cells. In addition, we examined the DNA-binding profiles of CTCF since it is required for both enhancer–promoter interactions and expression of MHC class II genes (10,11,16). CTCF binding sites were found to partition the MHC locus into domains that remain largely invariant over the first 6 h of IFN−γ treatment. However, an immediate change in genomic anchors was seen within 30 min of IFN−γ treatment, where they are recruited to CTCF binding sites and increase in number progressively up to 6 h. Collectively, these findings indicate that IFN−γ induces a rapid reconfiguration of the chromatin in the MHC at CTCF binding sites to poise the region for subsequent transcriptional activation.

MATERIALS AND METHODS

Cell culture and treatment

MRC5 lung fibroblasts were cultured in RPMI-1640 medium supplemented with 10% foetal calf serum and L-glutamine at 37°C in a 5% CO_2 atmosphere, and grown to 70% confluence. Cells were treated with 200 IU/ml of IFN−γ (recombinant human IFN-γ, R&D Systems) for 30 min or 6 h to induce transcriptional up-regulation in the MHC.

Isolation of genomic anchors

Genomic anchors were isolated from untreated and IFN−γ induced MRC5 cells using 2 M NaCl as described previously (17), except for the step of chromatin digestion which was carried out overnight with 600U Eco RI (Sigma), 600U HindIII (NEB), 200U HaeIII (NEB) and 40U BglII (NEB). DNA containing isolated genomic anchors was then purified and the concentration determined using a NanoDrop ND-1000. For each time point, three biological replicates were obtained, of which one was used for microarray hybridizations and two for RT-PCR validation.

Chromatin immunoprecipitation

Chromatin immunoprecipitation (ChIP) experiments were performed using untreated and IFN−γ induced MRC5 cells as described elsewhere (18). The experiments were performed using polyclonal antibodies against CTCF (Millipore 07-729) and BRG1 (Sigma SAB4200195). The chromatin was purified using a commercial purification kit (QIAmp DNA blood kit) and the DNA concentration determined using a NanoDrop ND-1000. Four biological replicates were obtained for each antibody, of which two were used for microarray hybridizations and two for the RT-PCR validation.

Array hybridization and data analysis

Purified DNA (500 ng) samples were labelled with Cy3- and Cy5-labelled dCTPs using the Agilent labelling kit and hybridized on custom made 244K genomic microarrays (Agilent) according to the manufacturer's protocol. This array platform contains 240 000 distinct 60-mer oligonucleotide probes spanning the entire MHC locus. The positions of the oligonucleotide probes were determined using the NCBI 36 build assembly of the human genome. The arrays were scanned on an Agilent Microarray Scanner G2565BA at 5 μm resolution. The data from ChIP-chip experiments were normalized with GeneSpring software. Briefly, a ratio of Cy5 to Cy3 fluorescent intensity (test signals/control signals) was calculated. For each channel, the median signals were subtracted from the median foreground signals. Log_2 ratios of test/control signal intensity were created and subsequently normalized by subtracting the weighted median for each array.

The NGS analyser (Genomatix) was applied for significant peak mining. NGS analyser parameters were set as following: (i) the size of the sliding window is 100 bp, (ii) the minimum number of reads per cluster (τ) was calculated from the data set applying a Poisson distribution (19). In order to reduce the possibility of false-positive peaks, the top 25% positive peaks were selected. A summary of the values obtained is shown in Supplementary Table S1. All the data from this study have been submitted to NCBI Gene Expression Omnibus (http://ncbi.nlm.nih.gov/geo/) under accession number GSE35845.

The four CTCF motifs were identified using MatInspector with a core similarity set to 0.75 and a matrix similarity set to 0.10 (20).

Validation of ChIP-chip data

PCR primers were designed using Primer 3 software (http://frodo.wi.mit.edu/cgi-bin/primer3/primer3_www.cgi). Real-time PCR was performed using SYBR Green Jumpstart Taq ReadyMix kit (Sigma Aldrich), 50 ng DNA and 2 μM primers using Opticon2 (MJ Research). For each primer pair, standard curves were constructed from real-time PCR reactions with known amounts of input DNA and used for product quantitation. Data analysis was performed using Opticon amplification detection software (MJ Research). The primer sequences used for the analysis are listed in Supplementary Table S2. The array enrichment of the selected sequences is shown in Supplementary Table S3.

RESULTS

Formation of new genomic anchors at the early stages of IFN-γ induction

Genomic anchors were isolated using 2 M NaCl extraction in MRC5 fibroblasts as previously reported (12,21–25),

and their positions identified by hybridization onto a high resolution 60-mer oligonucleotide tiling path microarray covering the entire MHC (Figure 1). Twenty-four genomic anchors were identified across the MHC in untreated fibroblasts, giving an average distribution of approximately one anchor every 160 kb. Nineteen anchors were present in the class I and classical class II regions, and the remaining five were within the class III and extended class II regions. Overall, 62% of the genomic anchors were located in intergenic regions, while 16% were in introns and 4% in exons. By 30-min treatment with IFN-γ, the number of genomic anchors had increased across the MHC ~5-fold to 124, giving an average of approximately one anchor every 30 kb. The greatest increase was present within the class II region. Anchors are characterized by AT tracts, topoisomerase binding sites and repetitive sequences (15,26,27). Here, we observed that 73% of anchors at 30 min IFN-γ treatment have repetitive sequences within 1 kb (data not shown). By 6 h, there was a substantial increase in genomic anchors to 270, giving an average of approximately one every 14 kb. Half of these were within the class II region, which constitutes 23% of the MHC locus but contains the largest number of IFN−γ inducible genes. In order to validate the findings, the presence or absence of genomic anchors at eight sites was confirmed using real-time PCR reactions on MRC5 cells at all three time points (Supplementary Figure S1).

While the inter- and intragenic distribution of genomic anchors was similar at all three time-points, more anchors were positioned closer to genes after IFN−γ treatment. Furthermore, ~72% of the anchors present at 30 min IFN-γ treatment are also present at 6 h. For example, at 30 min, *HLA-DRA* in the MHC class II region has genomic anchors at both its 5′ and 3′ ends. These remain at 6 h, but additional anchors are recruited closer to the gene body, as occurs at other IFN−γ inducible genes. The number of genomic anchors present within 2 kb of a transcription start site (TSS) in untreated cells across the MHC was 13, compared to 47 for 30 min and 107 for 6 h IFN−γ treatment, showing the same trend as our previous study on anchors in the MHC (12). All *HLA-DP*, *-DQ* and *–DR* genes have an anchored site within 2 kb of their TSS at 6 h.

Finally, we compared the genomic anchors identified here at 30 min and 6 h IFN-γ with those previously identified at 24 h (12). In the current study, we isolated genomic anchors using additional restriction enzymes and determined their distribution with a high resolution MHC microarray platform. The array contained heavily overlapping tiles of short oligonucleotides and excluded repetitive sequences. The arrays that were used in our previous study consisted of marginally overlapping tiles of 2 kb BACs, which contained repetitive as well as non-repetitive sequences. Despite these differences, 27.5 and 35.3% of anchors found in the class II region at 30 min and 6 h, respectively, are identical to those identified previously at 24 h (12). The distribution of anchors across the MHC and the trends observed upon IFN−γ induction are thus consistent between the different data sets.

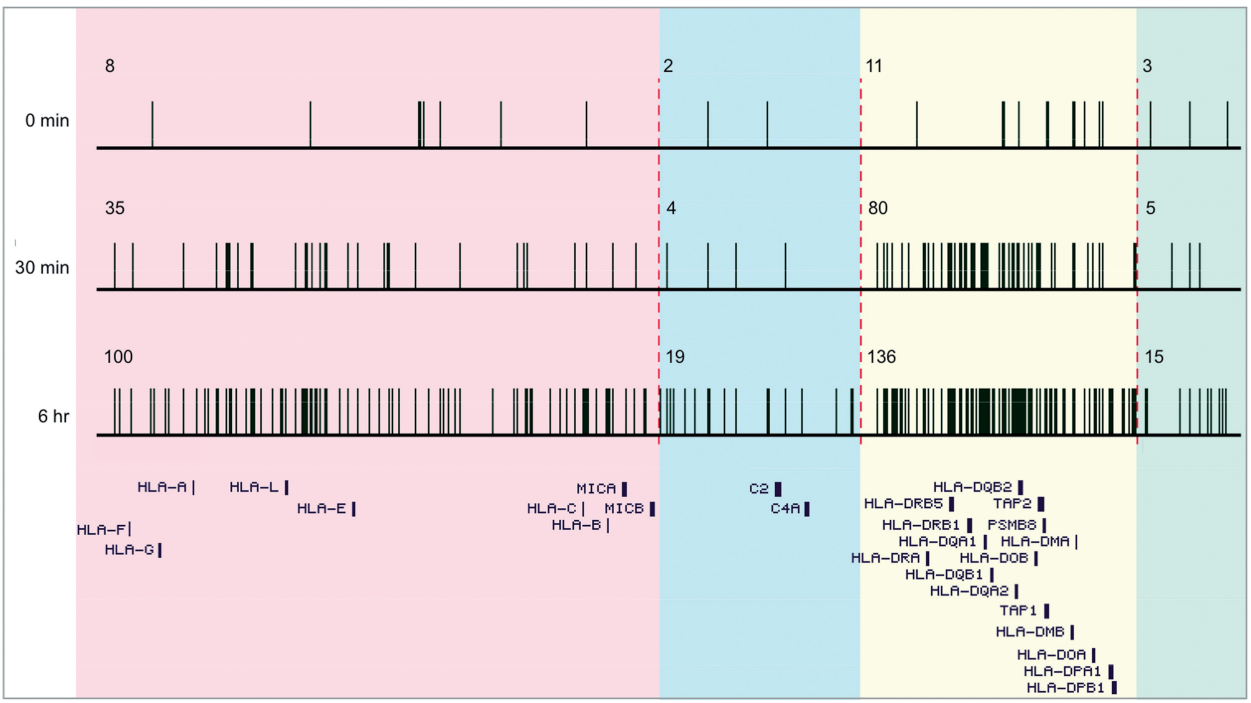

Figure 1. Genomic anchors in the MHC. The anchors were identified in untreated MRC5 fibroblasts, and fibroblasts induced for 30 min and 6 h with IFN−γ, using high resolution genomic tiling path arrays for the MHC. The number of genomic anchors in each region of the MHC is shown above the data plots. Selected RefSeq genes from the UCSC genome database (http://genome.ucsc.edu/) are shown below the array data. The different regions of the MHC are highlighted in different colours: classical class I, pink; classical class III, blue; classical class II, yellow; and extended class II, green. This colour scheme is used in subsequent figures.

Mapping of CTCF binding sites during IFN-γ activation

We then identified the binding sites of CTCF across the MHC in untreated MRC5 fibroblasts, and fibroblasts treated for 30 min and 6 h with IFN−γ, using ChIP combined with the high resolution microarrays described above (ChIP-chip) (Figure 2). Real-time PCR reactions were then performed to validate the findings (Supplementary Figure S1). In fibroblasts without IFN−γ, 65% of CTCF binding sites are clustered within the MHC class II region, 29% within the class I region and the remaining 6% within the class III and extended class II regions. Most CTCF sites are positioned within intergenic regions and are, on an average, 10 kb away from TSS. Unlike genomic anchors which increased in number upon IFN−γ treatment, CTCF binding sites were found to be generally unaffected at 30 min and 6 h with IFN–γ. This is in agreement with our previous study that showed that IFN–γ does not lead to transcriptional up-regulation of CTCF in fibroblasts (12).

A comparison between the CTCF sites in MRC5 cells and in different cell lines (data from ENCODE) are shown in Supplementary Table S4. Over 70% overlap is observed using a window size <5 kb. The discrepancies could be due to experimental differences as our MRC5 data are obtained using ChIP-chip while the ENCODE data are obtained using ChIP-seq. Cell-type specific differences could also explain the discrepancies, as seen for two cell lines in ENCODE, HUVEC and H1ESC, which show an overlap between their CTCF sites of ∼50%.

More than 75% of CTCF binding sites identified across the MHC in MRC5 fibroblasts contain four motifs which we have defined as CTCF-01, CTCF-02, CTCF-03 and CTCF-04 from the Genomatix transcription factor binding database, calculated from all known sites of interaction as a position weight matrix (28) (Figure 3). Three of the four motifs, CTCF-02, CTCF-03 and CTCF-04, contain the invariant consensus motif, CCnnnnGnnGGC, which was identified by Ohlson (2010) from computational analysis of CTCF motifs identified in several other studies (29). The majority of CTCF binding sites in MRC5 fibroblasts contain the CTCF-02 motif followed by CTCF-01, CTCF-03 and CTCF-04 (Supplementary Table S5). In contrast, 75% of reported CTCF binding sites in CD4, HeLa and Jurkat cells contain the CTCF-04 motif indicating cell-type differences (30).

A comparison with genomic anchors shows that in the absence of IFN−γ, there is no overlap between the positions of genomic anchors and sites bound by CTCF. However, following IFN−γ induction, the new genomic anchors are formed progressively at the genomic sites bound by CTCF. At 30 min IFN−γ, 45 genomic anchors have formed at CTCF binding sites and this number increases to 75 at 6 h (Figure 4). Further analysis indicates that the formation of genomic anchors upon IFN−γ induction at CTCF sites is statistically significant (Supplementary Table S6). These findings suggest that CTCF defines genomic regions that become reconfigured at the very early stages of MHC transcriptional up-regulation by IFN−γ.

XL9, a previously described region between *HLA-DRB1* and *HLA-DQA1*, is required for mediating promoter–enhancer loop interactions and expression of these MHC class II genes in Raji Burkitt's lymphoma B cells and in A431 epithelial cells after 12-h exposure to IFN−γ (10,31). We find that XL9 overlaps with sites that are stably bound by CTCF, and that the region progressively recruits genomic anchors at 30 min and 6 h (Figure 5). This critical regulatory region thus appears

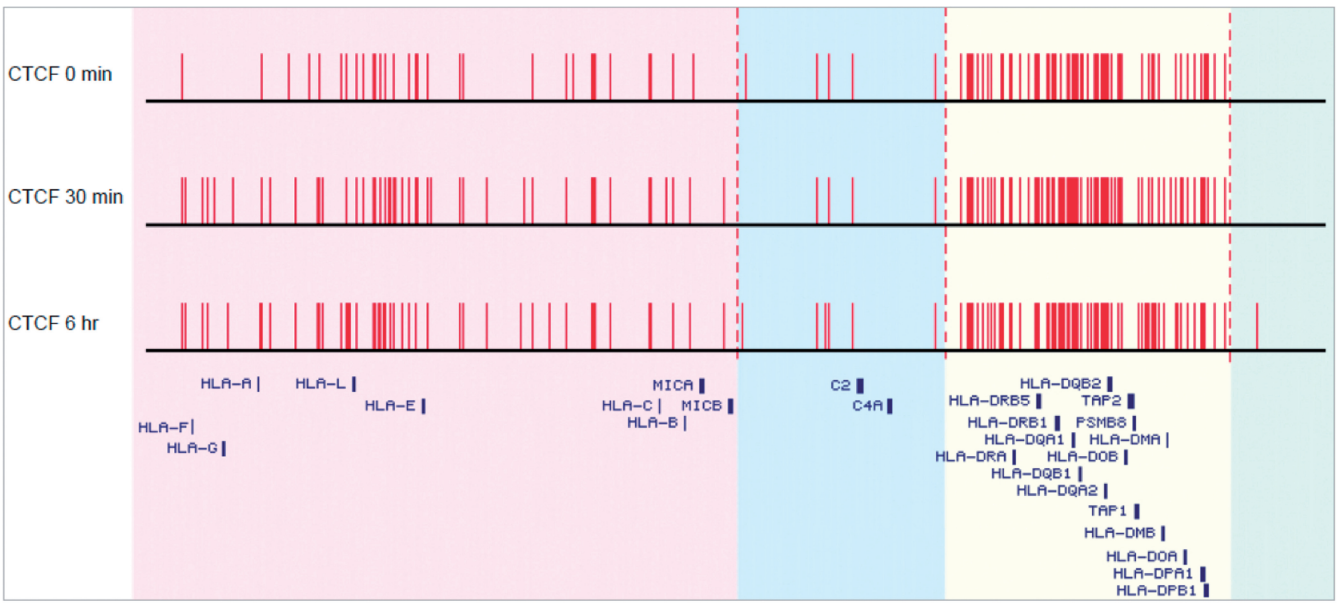

Figure 2. Genomic regions occupied by CTCF in the MHC. Sites bound by CTCF were identified in untreated MRC5 fibroblasts, and fibroblasts treated for 30 min and 6 h with IFN−γ, using a ChIP-chip-based approach. Colour scheme as in Figure 1.

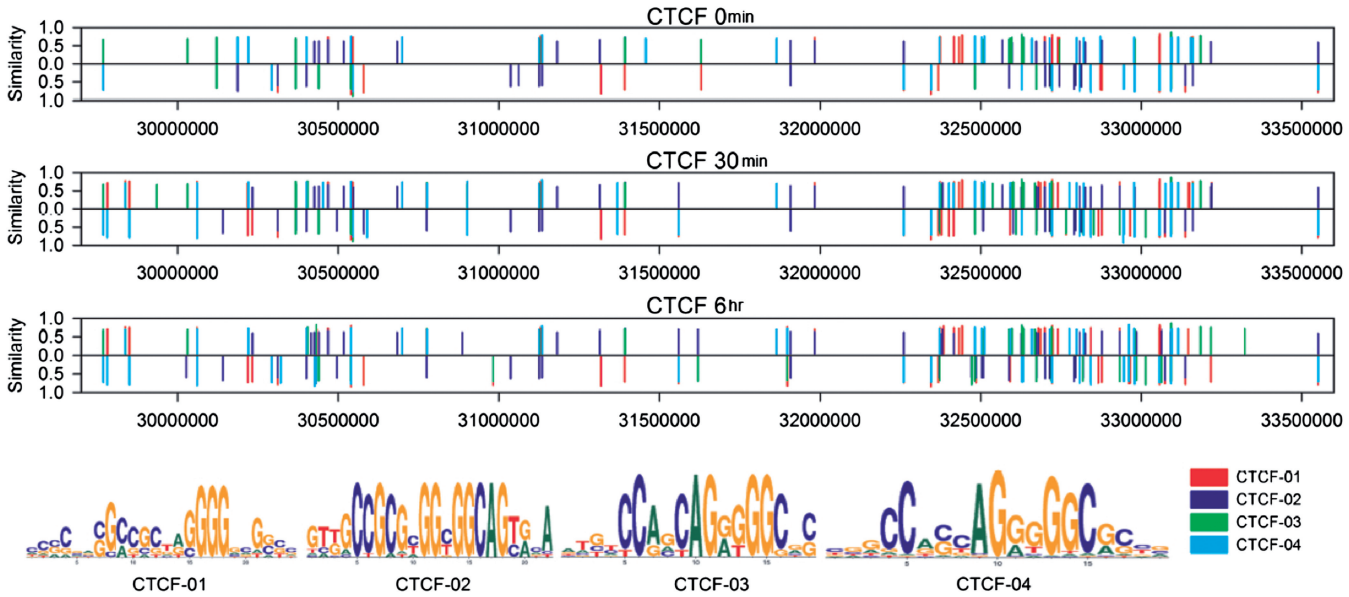

Figure 3. Distribution of four CTCF motifs within MHC regions occupied by CTCF. Bars above 0 represent genomic regions in the positive DNA strand while bars below 0 represent genomic regions in the negative DNA strand. The MHC is represented on the *x*-axis. The degree of similarity between the four CTCF motifs and the identified CTCF binding sites is represented on the *y*-axis. The sequence of the four CTCF motifs is also shown.

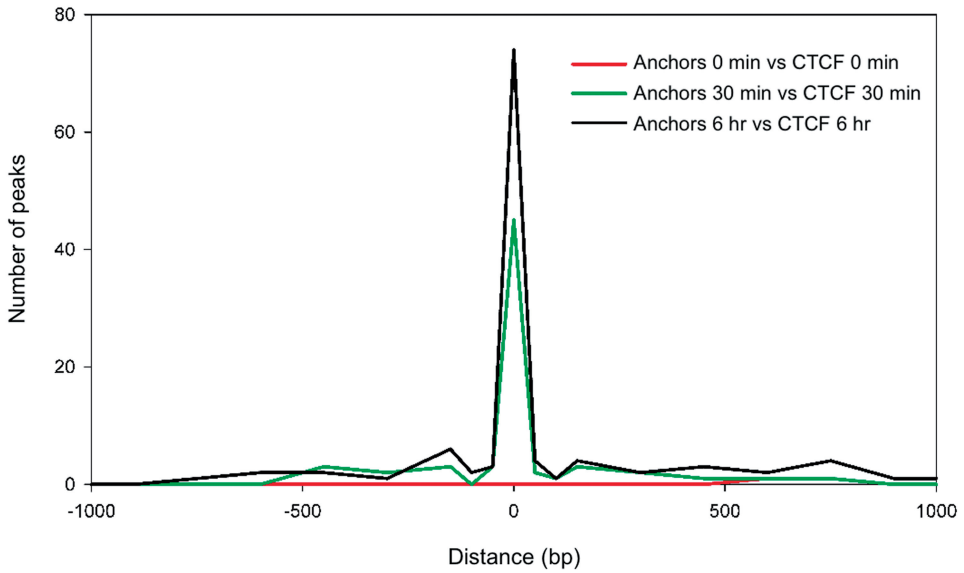

Figure 4. Genomic anchors are formed at CTCF sites upon IFN-γ induction. The analysis was performed using CTCF binding sites and genomic anchors in untreated MRC5 fibroblasts, and fibroblasts treated for 30 min and 6 h with IFN−γ. Midpoints of the binding sites were compared between the factors.

to mediate chromatin folding at the very early phases of IFN-γ induction.

Binding of BRG1 within domains defined by CTCF

BRG1, a component of the SWI/SNF ATP-dependent chromatin remodelling complex, is required for both IFN−γ dependent induction of CIITA (32,33) and the rapid formation of giant chromatin loops in the MHC (9). In order to determine whether the association of BRG1 with the MHC changes upon IFN−γ treatment, we conducted ChIP-chip experiments in untreated fibroblasts and fibroblasts treated with IFN−γ for 30 min. In untreated fibroblasts, BRG1 is present at high frequency, with 142, 64, 109 and 30 BRG1 binding sites found in the MHC class I, III, II and extended class II regions, respectively (Figure 6). Over 60% of these sites are located in intragenic regions or within 2 kb of a TSS. Ten of the 14 HLA genes in the MHC class II region have intragenic BRG1 binding sites, despite being transcriptionally silent.

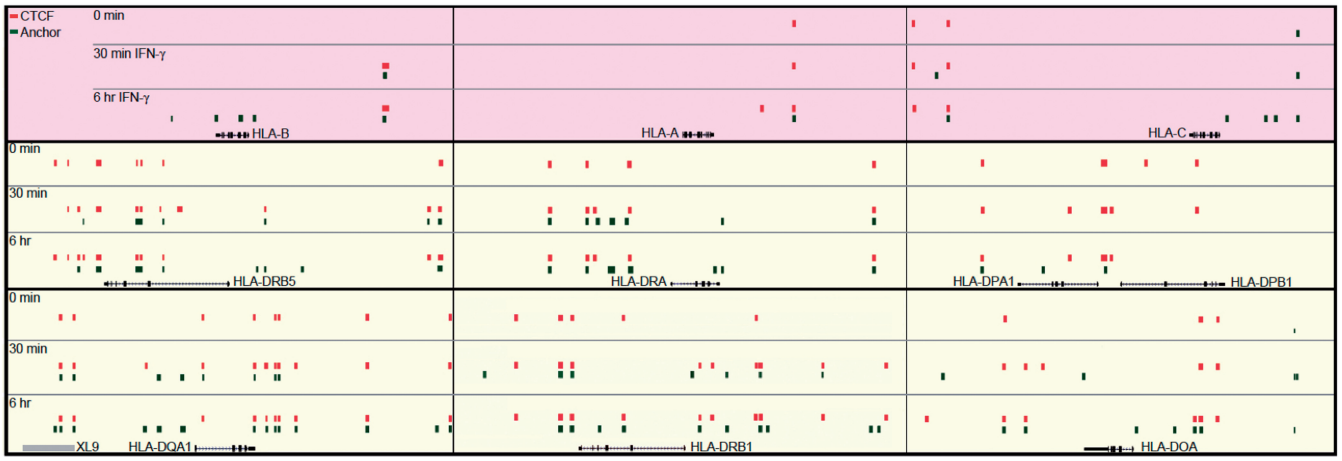

Figure 5. Genomic anchors are formed progressively with IFN-γ induction. The different elements are shown in MHC class I and class II genes in untreated MRC5 fibroblasts, and fibroblasts treated for 30 min and 6 h with IFN−γ. The genomic region XL9 is represented as a grey bar shown adjacent to the *HLA-DQA1* gene. Colour scheme as in Figure 1.

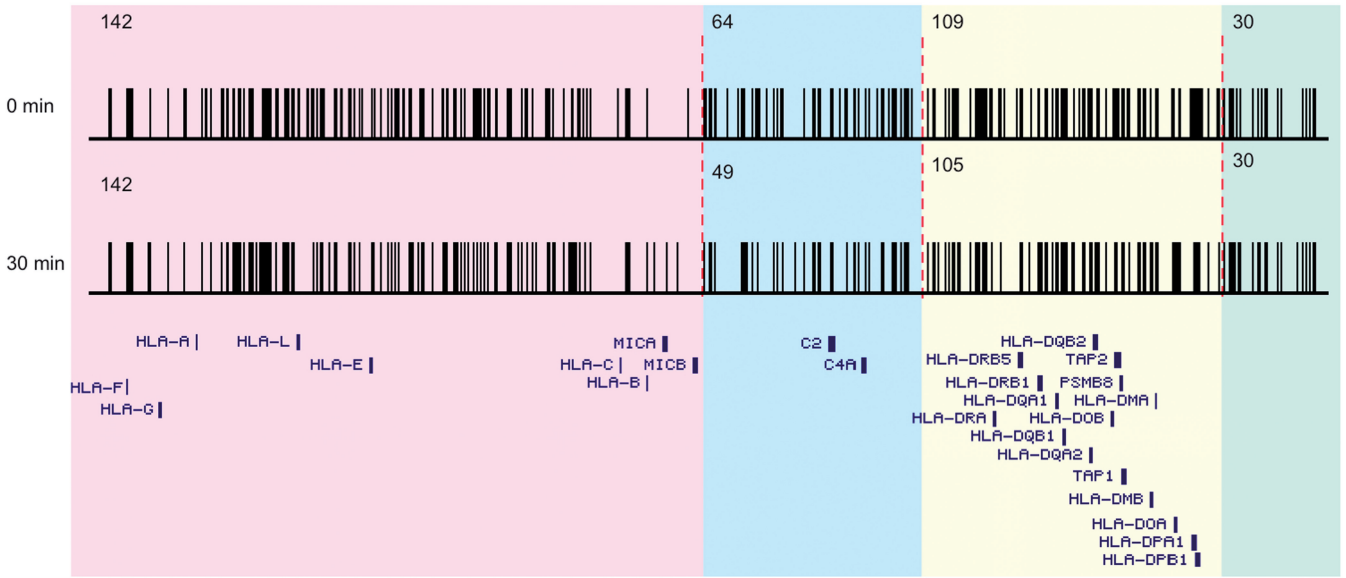

Figure 6. Genomic regions occupied by BRG1 in the MHC. Sites bound by BRG1 were identified in untreated fibroblasts, and fibroblasts treated for 30 min with IFN−γ. Colour scheme as in Figure 1.

The average distance of all BRG1 sites to a TSS is 5.6 kb. Less than 10% of BRG1 sites overlap with genomic anchors or CTCF sites, and the average distance between BRG1 and CTCF sites is 11 kb indicating a markedly different distribution. At 30 min of IFN−γ treatment, few changes are seen in BRG1 binding. Furthermore, no genomic anchors overlap with BRG1 binding sites in untreated fibroblasts and only two anchors overlap with BRG1 sites at 30 min of IFN−γ treatment (Supplementary Table S7).

DISCUSSION

In order to gain new insights into the molecular events in the MHC during the early stages of IFN−γ treatment, we examined the positions of genomic anchors and CTCF binding sites at 30 min IFN−γ treatment which coincides with the recruitment of phosphorylated STAT1 to the MHC (8,9), and at 6 h since it corresponds to the start of MHC class II gene expression under the influence of the MHC class II transactivator CIITA (7). In this study, we identified MHC sites which bind to CTCF and become rapidly reconfigured in fibroblasts at the start of IFN−γ induction. This reconfiguration is initiated independently of CIITA.

The number of genomic anchors in the MHC increases significantly during the first 30 min of IFN−γ treatment, and there is a further increase from 30 min to 6 h indicating progressive changes in higher order chromatin folding. In agreement with previous findings on IFN−γ-treated fibroblasts for 24 h (12), most of the new genomic anchors form at the early time points near

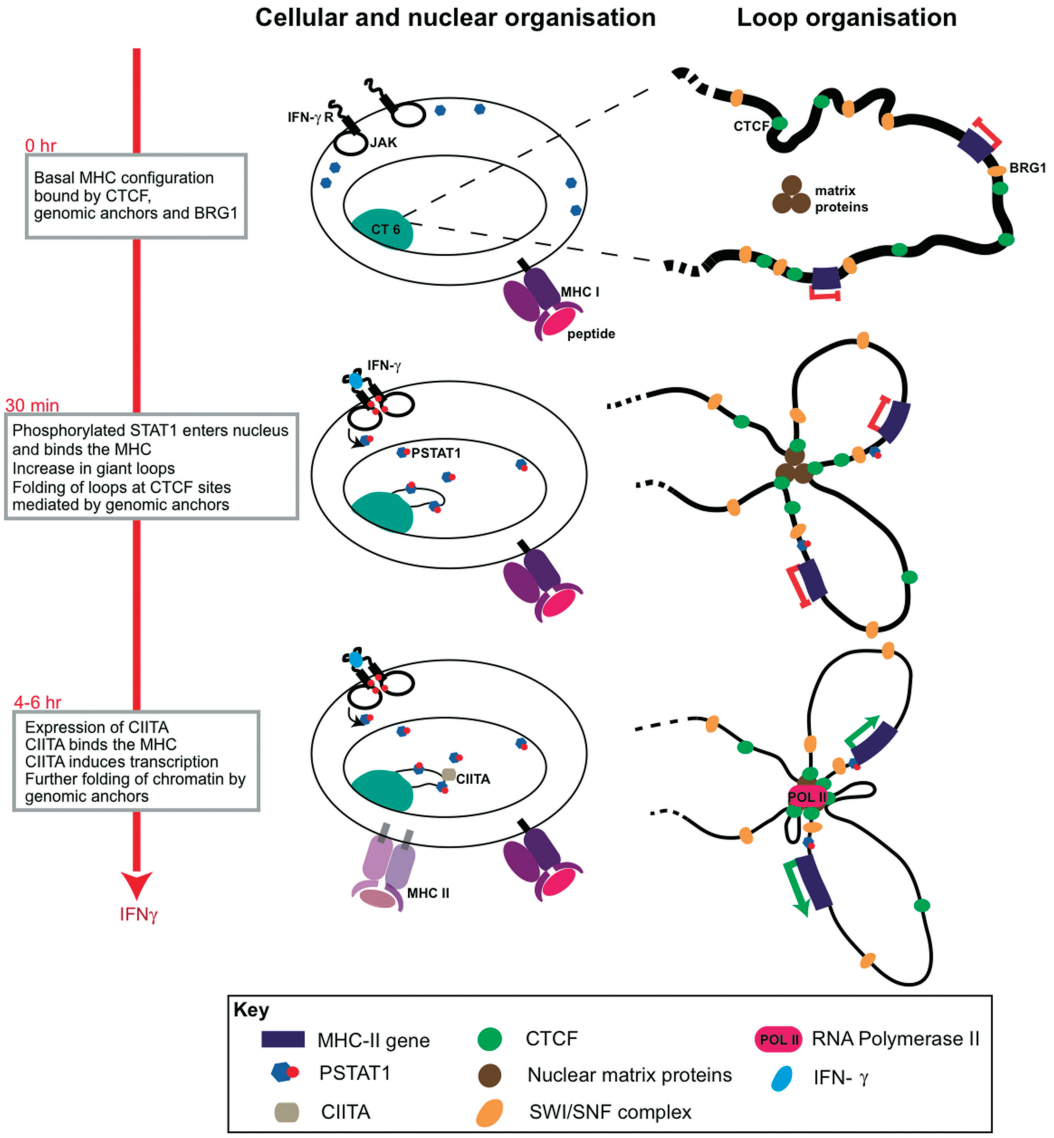

Figure 7. Model of chromatin organization during IFN−γ induced MHC class II expression in non-antigen presenting cells. The classical MHC class II genes, *HLA-DP*, *-DQ* and *-DR*, are not expressed in resting cells and the chromatin exists in a poised configuration. Stable CTCF-binding defines domains within the MHC, and BRG1 is constitutively associated with promoters and intergenic sequences. Upon activation of the IFN−γ receptor, phospho-STAT1 enters the nucleus and binds to DNA. Within 30 min, the chromatin configuration in the MHC is significantly altered by the formation of new genomic anchors at sites bound by CTCF. Chromatin folding is mediated by this process, and occurs in intergenic regions and proximal to promoter sequences. This is accompanied by the formation of giant chromatin loops and chromatin decondensation. Although BRG1 sites remain invariant, IFN−γ treatment promotes BRG1-dependent histone acetylation, which enhances sequence accessibility for DNA–protein interactions and chromatin flexibility for looping. This early step in IFN−γ primes the locus for transcription and is independent of CIITA, which is detected at HLA class II genes 4–6 h after the start of IFN−γ treatment. Further reconfiguration of genomic anchors occurs up to 6 h of IFN−γ exposure, to form an optimal platform for effective transcriptional induction of MHC class II genes.

IFN−γ-inducible genes in the MHC class II region. This region contains the greatest concentration of IFN−γ-regulated genes (1). The kinetics of these pre-transcriptional events is strikingly similar to that of giant chromatin loop formation (8) and suggests that the small and large-scale chromatin changes are linked. Environmental stimuli can thus lead to changes in chromatin architecture in the MHC several hours before the expression of CIITA and the MHC class II genes. The driver of these structural changes is likely to be the transcription factor STAT1, which is phosphorylated and enters the nucleus within minutes of the start of IFN−γ treatment (34). Support for this hypothesis is that in STAT1 negative cells, IFN−γ cannot induce up-regulation of transcription or the rapid formation of giant chromatin loops (9).

CTCF mediates promoter–enhancer interactions that are essential for both constitutive and inducible MHC class II expression (10,11,31). In agreement with the genome-wide distribution of CTCF (35), we observed that the MHC is bound extensively by CTCF. The distribution of CTCF binding sites is uneven across the

different MHC classes, since the majority cluster within the MHC class II region. Many of these binding sites are intergenic and, importantly, do not change in number or position with IFN−γ treatment indicating that CTCF defines distinct chromatin domains independent of transcription.

To determine whether CTCF binding sites are important at the very early stages of IFN−γ induction, we compared their positions with those of genomic anchors. In untreated fibroblasts, no anchors overlap with CTCF sites. At 30 min of IFN−γ treatment, new genomic anchors are formed at CTCF-binding sites and, by 6 h, they increase substantially in number. IFN−γ treatment thus induces a rapid reconfiguration of chromatin at genomic sites occupied by CTCF. Experiments using CTCF-negative cells could reveal whether the protein is required for the rapid formation of genomic anchors upon IFN−γ induction. Studies at the imprinted locus Igf2/H19 show that CTCF interacts with a genomic anchor to form a looped chromatin structure (36). Our findings suggest that the dynamic interactions between CTCF and genomic anchors change the topology of the MHC locus and demarcate new domains required for transcription. It has also been shown that CTCF mediates interchromosomal colocalization of Igf2/H19 and Wsb1/Nf1 (37). It is thus tempting to speculate that the interaction of CTCF with genomic anchors is required for the relocalization of the MHC in a transcriptionally permissive nuclear microenvironment.

BRG1 binding sites are stable over the first 30 min of IFN-γ induction and do not overlap with either genomic anchors or CTCF-binding sites. This is consistent with its previous description as invariant upon IFN−γ induction at the CIITA gene locus, although it is essential for chromatin loop reorganization and CIITA expression (9,32,33). In a recent genome-wide study of BRG1 binding sites in stimulated and unstimulated CD4+ T helper cell subsets (naïve, Th1 and Th2), the majority of binding sites were conserved across the cell types and one-quarter were unique to each cell subset (38). BRG1 binding did not correlate with expression, and at prototypical T-cell lineage loci there was almost identical binding of BRG1 in Th1 and Th2 cells (38). Taken together, these findings suggest that the stable association of BRG1 facilitates efficient chromatin remodelling in the MHC within domains defined by CTCF and genomic anchors.

We thus propose a model for the early stages of MHC class II activation by IFN−γ in non-antigen presenting cells (Figure 7). Poised for activation, the MHC is compartmentalized by CTCF and is constitutively bound by BRG1. Within 30 min of IFN−γ exposure, phospho-STAT1 enters the nucleus and chromatin starts to be reconfigured at sites occupied by CTCF to form chromatin hubs. This process occurs independently of CIITA. Further modification of chromatin architecture occurs up to 6 h of IFN−γ exposure to form an optimal platform for effective and coordinate expression of MHC class II genes.

ACCESSION NUMBERS

GSE35845.

SUPPLEMENTARY DATA

Supplementary Data are available at NAR Online: Supplementary Tables 1–7 and Supplementary Figure 1.

ACKNOWLEDGEMENTS

We are grateful to Doug King for his help with the microarray hybridizations.

FUNDING

Cancer Research UK programme grant C5321/A8318 (to D.S.) and NICHD grant HD36512 (to S.A.K.). Funding for open access charge: Cancer Research UK programme grant C5321/A8318.

Conflict of interest statement. None declared.

REFERENCES

1. Horton,R., Wilming,L., Rand,V., Lovering,R.C., Bruford,E.A., Khodiyar,V.K., Lush,M.J., Povey,S., Talbot,C.C. Jr, Wright,M.W. *et al*. (2004) Gene map of the extended human MHC. *Nat Rev Genet*, **5**, 889–899.
2. Trowsdale,J. (2011) The MHC, disease and selection. *Immunol. Lett*, **137**, 1–8.
3. Trowsdale,J. (2002) The gentle art of gene arrangement: the meaning of gene clusters. *Genome Biol*, **3**, COMMENT2002.1–COMMENT2002.5.
4. Reith,W., LeibundGut-Landmann,S. and Waldburger,J.M. (2005) Regulation of MHC class II gene expression by the class II transactivator. *Nat. Rev. Immunol.*, **5**, 793–806.
5. Young,H.A. and Bream,J.H. (2007) IFN-gamma: recent advances in understanding regulation of expression, biological functions, and clinical applications. *Curr. Top. Microbiol. Immunol.*, **316**, 97–117.
6. Zika,E. and Ting,J.P. (2005) Epigenetic control of MHC-II: interplay between CIITA and histone-modifying enzymes. *Curr. Opin. Immunol.*, **17**, 58–64.
7. Rybtsova,N., Leimgruber,E., Seguin-Estévez,Q., Dunand-Sauthier,I., Krawczyk,M. and Reith,W. (2007) Transcription-coupled deposition of histone modifications during MHC class II gene activation. *Nucleic Acids Res.*, **35**, 3431–3441.
8. Volpi,E.V., Chevret,E., Jones,T., Vatcheva,R., Williamson,J., Beck,S., Campbell,R.D., Goldsworthy,M., Powis,S.H., Ragoussis,J. *et al*. (2000) Large-scale chromatin organization of the major histocompatibility complex and other regions of human chromosome 6 and its response to interferon in interphase nuclei. *J. Cell. Sci.*, **113**, 1565–1576.
9. Christova,R., Jones,T., Wu,P.J., Bolzer,A., Costa-Pereira,A.P., Watling,D., Kerr,I.M. and Sheer,D. (2007) P-STAT1 mediates higher-order chromatin remodelling of the human MHC in response to IFNgamma. *J. Cell. Sci.*, **120**, 3262–3270.
10. Majumder,P., Gomez,J.A., Chadwick,B.P. and Boss,J.M. (2008) The insulator factor CTCF controls MHC class II gene expression and is required for the formation of long-distance chromatin interactions. *J. Exp. Med.*, **205**, 785–798.
11. Majumder,P. and Boss,J.M. (2010) CTCF controls expression and chromatin architecture of the human major histocompatibility complex class II locus. *Mol. Cell. Biol.*, **30**, 4211–4223.
12. Ottaviani,D., Lever,E., Mitter,R., Jones,T., Forshew,T., Christova,R., Tomazou,E.M., Rakyan,V.K., Krawetz,S.A., Platts,A.E. *et al*. (2008) Reconfiguration of genomic anchors upon

transcriptional activation of the human major histocompatibility complex. *Genome Res.*, **18**, 1778–1786.
13. Cai,S., Lee,C.C. and Kohwi-Shigematsu,T. (2006) SATB1 packages densely looped, transcriptionally active chromatin for coordinated expression of cytokine genes. *Nat. Genet.*, **38**, 1278–1288.
14. Kumar,P.P., Bischof,O., Purbey,P.K., Notani,D., Urlaub,H., Dejean,A. and Galande,S. (2007) Functional interaction between PML and SATB1 regulates chromatin-loop architecture and transcription of the MHC class I locus. *Nat. Cell. Biol.*, **9**, 45–56.
15. Ottaviani,D., Lever,E., Takousis,P. and Sheer,D. (2008) Anchoring the genome. *Genome Biol.*, **9**, 201.
16. Klenova,E.M., Morse,H.C. 3rd, Ohlsson,R. and Lobanenkov,V.V. (2002) The novel BORIS + CTCF gene family is uniquely involved in the epigenetics of normal biology and cancer. *Semin. Cancer Biol.*, **12**, 399–414.
17. Krawetz,S.A., Draghici,S., Goodrich,R., Liu,Z. and Ostermeier,G.C. (2005) In silico and wet-bench identification of nuclear matrix attachment regions. *Methods Mol. Med.*, **108**, 439–458.
18. Christova,R. and Oelgeschlager,T. (2002) Association of human TFIID-promoter complexes with silenced mitotic chromatin in vivo. *Nat. Cell. Biol.*, **4**, 79–82.
19. Sultan,M., Schulz,M.H., Richard,H., Magen,A., Klingenhoff,A., Scherf,M., Seiferth,M., Borodina,T., Soldatov,A., Parkhomchuk,D. *et al.* (2008) A global view of gene activity and alternative splicing by deep sequencing of the human transcriptome. *Science*, **321**, 956–960.
20. Cartharius,K., Frech,K., Grote,K., Klocke,B., Haltmeier,M., Klingenhoff,A., Frisch,M., Bayerlein,M. and Werner,T. (2005) MatInspector and beyond: promoter analysis based on transcription factor binding sites. *Bioinformatics*, **21**, 2933–2942.
21. Dunn,K.L., Zhao,H. and Davie,J.R. (2003) The insulator binding protein CTCF associates with the nuclear matrix. *Exp. Cell Res.*, **288**, 218–223.
22. Yusufzai,T.M. and Felsenfeld,G. (2004) The 5′-HS4 chicken beta-globin insulator is a CTCF-dependent nuclear matrix-associated element. *Proc. Natl Acad. Sci. USA*, **101**, 8620–8624.
23. Linnemann,A.K. and Krawetz,S.A. (2009) Silencing by nuclear matrix attachment distinguishes cell-type specificity: association with increased proliferation capacity. *Nucleic Acids Res.*, **37**, 2779–2788.
24. Linnemann,A.K., Platts,A.E. and Krawetz,S.A. (2009) Differential nuclear scaffold/matrix attachment marks expressed genes. *Hum. Mol. Genet.*, **18**, 645–654.
25. Drennan,K.J., Linnemann,A.K., Platts,A.E., Heng,H.H., Armant,D.R. and Krawetz,S.A. (2010) Nuclear matrix association: switching to the invasive cytotrophoblast. *Placenta*, **31**, 365–372.
26. Platts,A.E., Quayle,A.K. and Krawetz,S.A. (2006) In-silico prediction and observations of nuclear matrix attachment. *Cell. Mol. Biol. Lett.*, **11**, 191–213.
27. Liebich,I., Bode,J., Reuter,I. and Wingender,E. (2002) Evaluation of sequence motifs found in scaffold/matrix-attached regions (S/MARs). *Nucleic Acids Res.*, **30**, 3433–3442.
28. Krawetz,S. and Werner,T. (2009) *Bioinformatics for Systems Biology*. Humana Press, New York, pp. 339–352.
29. Ohlsson,R., Lobanenkov,V. and Klenova,E. (2010) Does CTCF mediate between nuclear organization and gene expression? *Bioessays*, **32**, 37–50.
30. Cuddapah,S., Jothi,R., Schones,D.E., Roh,T.Y., Cui,K. and Zhao,K. (2009) Global analysis of the insulator binding protein CTCF in chromatin barrier regions reveals demarcation of active and repressive domains. *Genome Res.*, **19**, 24–32.
31. Majumder,P., Gomez,J.A. and Boss,J.M. (2006) The human major histocompatibility complex class II HLA-DRB1 and HLA-DQA1 genes are separated by a CTCF-binding enhancer-blocking element. *J. Biol. Chem.*, **281**, 18435–18443.
32. Ni,Z., Karaskov,E., Yu,T., Callaghan,S.M., Der,S., Park,D.S., Xu,Z., Pattenden,S.G. and Bremner,R. (2005) Apical role for BRG1 in cytokine-induced promoter assembly. *Proc. Natl Acad. Sci. USA*, **102**, 14611–14616.
33. Ni,Z., Abou El Hassan,M., Xu,Z., Yu,T. and Bremner,R. (2008) The chromatin-remodeling enzyme BRG1 coordinates CIITA induction through many interdependent distal enhancers. *Nat. Immunol.*, **9**, 785–793.
34. Lillemeier,B.F., Koster,M. and Kerr,I.M. (2001) STAT1 from the cell membrane to the DNA. *EMBO J.*, **20**, 2508–2517.
35. Kim,T.H., Abdullaev,Z.K., Smith,A.D., Ching,K.A., Loukinov,D.I., Green,R.D., Zhang,M.Q., Lobanenkov,V.V. and Ren,B. (2007) Analysis of the vertebrate insulator protein CTCF-binding sites in the human genome. *Cell*, **128**, 1231–1245.
36. Kurukuti,S., Tiwari,V.K., Tavoosidana,G., Pugacheva,E., Murrell,A., Zhao,Z., Lobanenkov,V., Reik,W. and Ohlsson,R. (2006) CTCF binding at the H19 imprinting control region mediates maternally inherited higher-order chromatin conformation to restrict enhancer access to Igf2. *Proc. Natl Acad. Sci. USA*, **103**, 10684–10689.
37. Ling,J.Q., Li,T., Hu,J.F., Vu,T.H., Chen,H.L., Qiu,X.W., Cherry,A.M. and Hoffman,A.R. (2006) CTCF mediates interchromosomal colocalization between Igf2/H19 and Wsb1/Nf1. *Science*, **312**, 269–272.
38. De,S., Wurster,A.L., Precht,P., Wood,W.H. 3rd, Becker,K.G. and Pazin,M.J. (2011) Dynamic BRG1 recruitment during T helper differentiation and activation reveals distal regulatory elements. *Mol. Cell. Biol.*, **7**, 1512–1527.